



**HAL**  
open science

# Radar Cross Section estimation of a set of randomly distributed dipoles as an application to RFiD in a high density context

Aiman Mughal, Benoit Poussot, Shermila Mostarshedi, Jithin  
Mudakkarappilli Sudersanan, Jean-Marc Laheurte

## ► To cite this version:

Aiman Mughal, Benoit Poussot, Shermila Mostarshedi, Jithin Mudakkarappilli Sudersanan, Jean-Marc Laheurte. Radar Cross Section estimation of a set of randomly distributed dipoles as an application to RFiD in a high density context. 8th International Conference on Antennas and Electromagnetic Systems (AES), May 2022, Marrakesh, Morocco. hal-04047437

**HAL Id: hal-04047437**

**<https://hal.science/hal-04047437>**

Submitted on 4 Jul 2023

**HAL** is a multi-disciplinary open access archive for the deposit and dissemination of scientific research documents, whether they are published or not. The documents may come from teaching and research institutions in France or abroad, or from public or private research centers.

L'archive ouverte pluridisciplinaire **HAL**, est destinée au dépôt et à la diffusion de documents scientifiques de niveau recherche, publiés ou non, émanant des établissements d'enseignement et de recherche français ou étrangers, des laboratoires publics ou privés.

# Radar Cross Section estimation of a set of randomly distributed dipoles as an application to RFID in a high density context

Aiman Mughal\*, Jithin Mudakkarappilli Sudersanan\*, Shermila Mostarshedi,  
Benoit Poussot, Jean-Marc Laheurte

ESYCOM Lab, Univ Gustave Eiffel, CNRS, F-77454 Marne-la-vallee, France

\*E-mail: [aiman.mughal@univ-eiffel.fr](mailto:aiman.mughal@univ-eiffel.fr), [jithin.mudakkarappilli-sudersanan@univ-eiffel.fr](mailto:jithin.mudakkarappilli-sudersanan@univ-eiffel.fr)

## Abstract

Randomly distributed RFID tags are modeled by a set of short-circuited half-wave dipoles. Numerical Electromagnetics Code (NEC) simulator is used for the computation of mono-static radar cross section (RCS) following the two techniques based on the total field backscattered by the target and the radar equation. Different dipole configurations are studied to highlight the RCS distortion. The radar equation makes it possible to estimate RCS from measurements. The simulation results were found to be in good agreement with the experimental data.

**Keywords:** backscattered field, electromagnetic coupling, radar equation, mono-static RCS measurements

## 1. Introduction

RFID (Radio Frequency Identification) technology is widely deployed in several frequency bands and for different applications such as logistics, inventory tracking, supply-chain management and laundry management [1]. A passive UHF RFID system is composed of a tag and a reader, where the tag contains an antenna and an integrated circuit (the chip). The passive tag is powered up by the electromagnetic field received from the reader. The communication link between the reader and the tag is established by switching its chip impedance between two distinct states, resulting in a modulation of the signal scattered back towards the reader. The backscattered field of the tag can be analyzed in terms of its radar cross section.

Mono-static RCS is a key parameter used to assess the quality of an RFID communication link. Impedance matching between the tag antenna and the chip directly influences the RCS and thereby the performance parameters of the RFID system, such as read-range and read-rate. In high-density context, the tags are randomly distributed over a specified surface area which may result in significant electromagnetic coupling among them. This causes the radiation properties of an RFID tag to undergo random variations, which may be different from one configuration to another. Although the estimation of RCS in deterministic cases has been largely studied in literature [2], [3], to our knowledge the impact of introducing randomness in the system has not yet been studied.

The manuscript is organized as follows: in Section 2, an RFID system consisting of a set of  $N$  randomly distributed tags over an electrically small area, is modeled by a set of dipoles. Section 3 presents the two approaches used in this paper to compute the mono-static RCS of an RFID system and also NEC simulations to compute RCS for uniform and random configuration of dipoles. Simulation results are validated by measurements as discussed in section 4.

## 2. Dipole-based model for an RFID system

Figure 1(a) presents an RFID system consisting of a random distribution of  $N$  tags over a specific area in the  $yoz$  plane, illuminated by a reader positioned at a point in space (here on the  $x$ -axis).

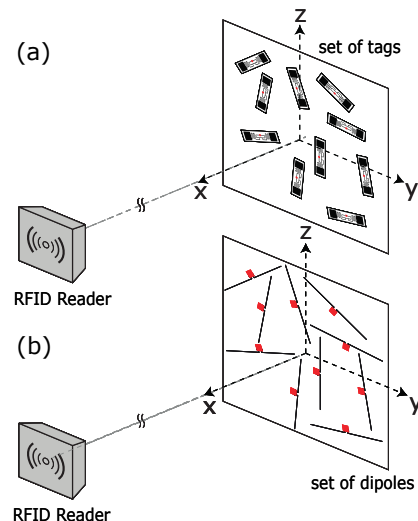


Figure 1: Set of RFID tags illuminated by the reader in (a) is modeled by a set of dipoles in (b)

The tag centers are assumed to be randomly distributed such that they do not overlap. On account of the statistical similarities discussed in [6], the tag antennas are modeled by half-wave dipoles. The dipoles representing the tags are loaded. The centers and orientations of the  $N$  dipoles are supposed to be the same as that of the randomly distributed tags. Thereby, it is assumed that studying the mono-static RCS of the set of  $N$  dipoles in Figure 1(b) could statistically represent the RCS of the  $N$  tags.

### 3. Mono-static radar cross section

The mono-static RCS ( $\sigma$ ) in  $\text{dBm}^2$  of a set of randomly distributed loaded dipoles acting as the target, is computed using the two methods explained in this section.

#### 3.1. RCS using backscattered field

The reader antenna illuminates the dipoles (target) with an incident electromagnetic field ( $E_i$ ). This field induces a voltage at the input of each of the dipoles which generates a backscattered field ( $E_s$ ) in all directions. The total mono-static RCS from the set of dipoles is then calculated in the direction of the incident electromagnetic field by [4]:

$$\sigma = \lim_{r \rightarrow +\infty} 4\pi r^2 \frac{|E_s|^2}{|E_i|^2} \quad (1)$$

where  $r$  is the distance between the reader and target.

#### 3.2. RCS using radar equation

The RCS can be determined from measurements in terms of the reflection coefficient by using the radar equation. The measurements are performed in an anechoic chamber by placing the dipoles (target) in the far-field of the transmitting horn antenna (reader). The reflection coefficient of the reader is measured in the presence and absence of the target. Following the detailed calculations in [5], RCS could be calculated using:

$$\sigma = |S_{11}^{+\text{target}} - S_{11}^{-\text{target}}|^2 \frac{(4\pi)^3 r^4}{G_t^2 \lambda^2} \quad (2)$$

where  $S_{11}^{+\text{target}}$  and  $S_{11}^{-\text{target}}$  are the reflection coefficients

of the reader with and without the target respectively,  $G_t$  is the realized gain of the reader in free space including the mismatch losses, and  $r$  is the distance between the reader and the target.

#### 3.3. Simulation results

NEC is used to simulate both approaches for the calculation of RCS. for the first approach, in order to estimate the backscattered field, a planewave is implemented in NEC. For the second approach, in order to use the radar equation, the reader is modeled by an excited dipole to create the incident electromagnetic field in order to illuminate the set of dipoles. We consider thin short-circuited ( $Z_c = 0$ ) dipoles of length  $\lambda/2$  and diameter  $10^{-6}\lambda$  at an operating frequency of 866 MHz. Figure 2 presents the estimated RCS of an isolated dipole in (a) and of a configuration of two dipoles separated by a distance of  $d = 0.2\lambda$ , where one of them is inclined at an angle of  $20^\circ$  as shown in (b).

The two techniques show an excellent agreement in both cases. It is observed that the RCS of the second configuration presents a distorted form and different angular values for three planes ( $\phi = 0^\circ$ ,  $\phi = 90^\circ$ , and  $\theta = 90^\circ$ ) in comparison with that of the isolated case. This distortion is more visibly observed in  $\phi = 90^\circ$  plane, which leads us to investigate RCS in this plane by performing measurements. The two NEC-based methods discussed in this section can be used as a reference for the evaluation of the RCS in different dipole configurations (periodic and random). Further analysis on the distortion of RCS for random orientation of dipoles is done through experimental validation, especially in the case of a set of highly coupled dipoles (cf. Fig. 1).

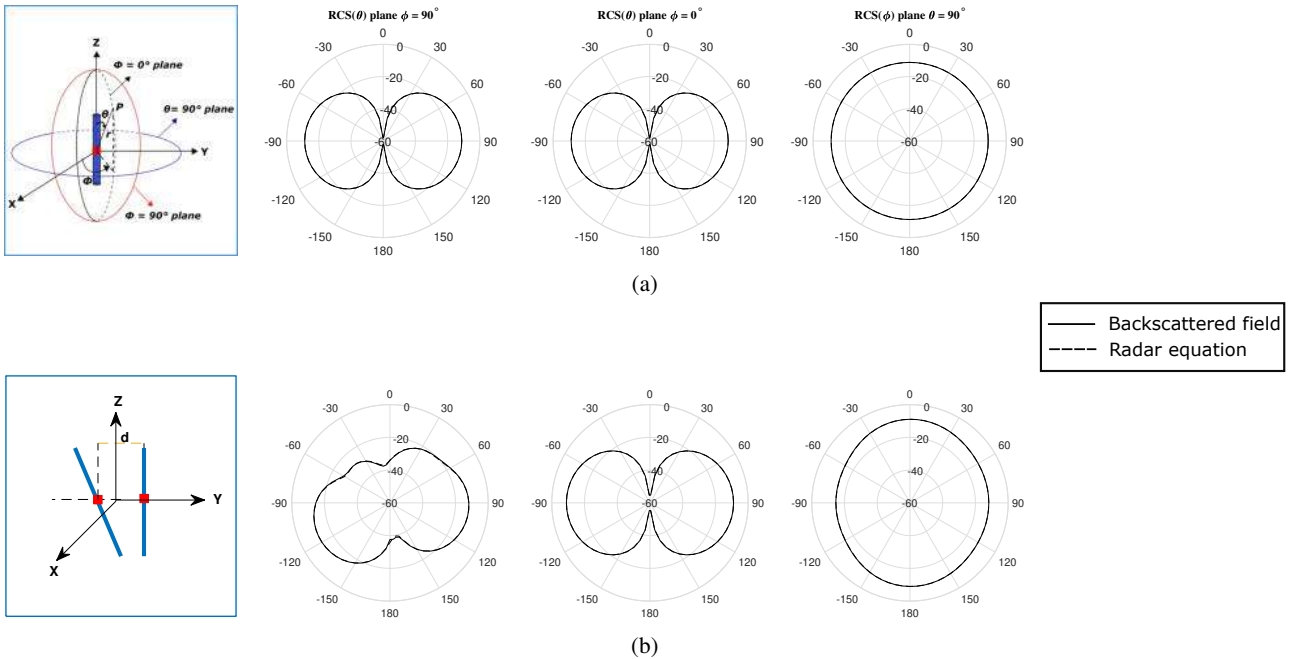


Figure 2: Mono-static RCS in three different planes ( $\phi = 90^\circ$ ,  $\phi = 0^\circ$  and  $\theta = 90^\circ$ ) for an isolated dipole in (a) and two dipoles with one inclined at  $20^\circ$  in (b)

## 4. RCS measurements

### 4.1. Measurement setup

This section elucidates the single-port network analyzer measurement used for estimating mono-static RCS in an anechoic chamber [2], [5]. A schematic representation of the measurement setup is shown in Figure 3.

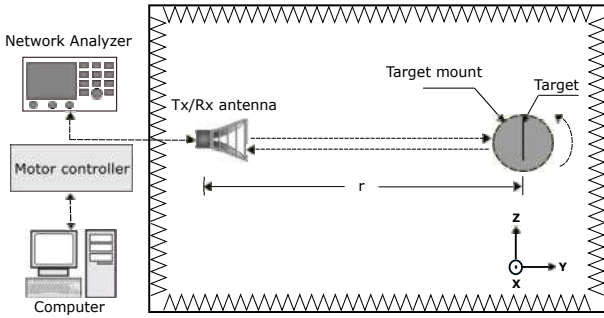


Figure 3: Experimental setup for measuring mono-static RCS in anechoic chamber

The measurement bench consists of E8361C PNA Microwave Network Analyzer (10 MHz - 67 GHz), a dual ridge horn antenna SH800 with an operational frequency range of 0.8 - 12 GHz acting as the Tx/Rx antenna, and a stepped motor which controls the rotation of the target mount. The target is mounted on a foam support to avoid any unwanted reflections which could interfere with the desired reflections from the target. The distance ( $r$ ) between the Tx/Rx antenna and the target is fixed to 2.6 m, complying with the far-field conditions. It is measured from the input port of the Tx/Rx antenna to the center of the target mount. Only horizontal polarization of the antenna is em-

ployed as the study focuses on the  $\phi = 90^\circ$  plane. The key parameters used for measurements using the network analyzer is summarized in Table 1.

Parameter	Value used
Frequency range	0.8 - 4 GHz
IF bandwidth	5 kHz
Number of points	25601
Input power	7 dBm
Average factor	10

Table 1: Basic setup parameters used in network analyzer

The measurement procedure is carried out in two stages. First, the reflection coefficient of the reader antenna is measured in the absence of the target ( $S_{11}^{-\text{target}}$ ). The measured value includes the effect of input port mismatch and unwanted reflections inside the anechoic chamber. Subsequently, the target is placed on the mount and the reflection coefficient ( $S_{11}^{+\text{target}}$ ) is measured.

Data pre-processing techniques are employed to eliminate systematic errors from the measured data to obtain the correct RCS of the target [7], [8]. S-parameter calibration is performed at first to suppress errors of the measurement path, namely the PNA and cable connected to the Tx/Rx antenna. A background vector subtraction technique is used to coherently subtract the backscattered signals from the test range with and without the presence of the target, in order to eliminate effects of the background. Any residual reflections that remain from the background subtraction are filtered out using the time gating technique employing a suitable window. Kaiser-Bessel window is used in the context of this work. The parameter ( $K = 4$ ) of the window is

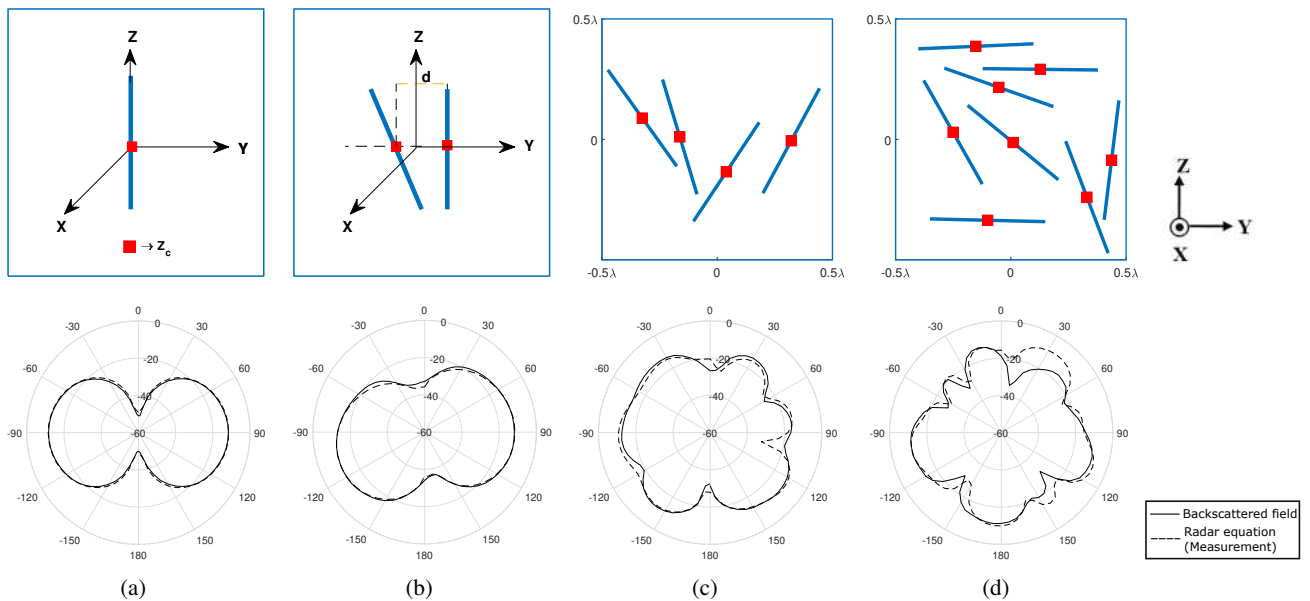


Figure 4: Mono-static RCS in  $\phi = 90^\circ$  plane for an isolated dipole in (a), two dipoles with one tilted at  $20^\circ$  in (b), a set of four randomly distributed dipoles in (c), and a set of eight randomly distributed dipoles in (d)

chosen so as to have sufficient suppression in the side lobe level. The width of time gate (gate span = 1.68 m) is chosen such that it covers the peak corresponding to the target.

## 4.2. Measurement results

Mono-static RCS of thick short-circuited ( $Z_c = 0$ ) dipoles of length  $\lambda/2$  and diameter of 1 mm is measured at the frequency of 866 MHz. The choice of short-circuit load is justified by the simplicity of its implementation for a preliminary study. The measurement results are compared with those obtained by the NEC electromagnetic simulator following the technique described in section 2.a. Figure 4 presents the results of the RCS for a few different configurations and a good agreement is observed between the measurements and the simulations in  $\phi = 90^\circ$  plane. It is observed that the RCS of an isolated dipole gets deformed when a second dipole inclined at  $20^\circ$  is introduced at a distance  $d = 40$  mm from it. Furthermore, the total RCS in the case of a set of 4 and 8 randomly distributed dipoles are measured and analyzed. The dipoles are distributed over a surface area of  $1\lambda \times 1\lambda$ . The results are more distorted and totally perturbed in the case of 4 and 8 dipoles.

The difference between the measured and simulated results could be potentially arising from the slight misalignment in position of dipoles on the plane and minor variations in the dipole lengths. Moreover, background subtraction followed by time gating may not suppress all errors. Even though the window function has a width covering most of the target reflection. There is not always a clear border of the target response while performing gating. In such a case, some part of the desired target response could be lost or some unwanted responses could be included in the time-gated signal, resulting in variations in the RCS response.

## 5. Conclusion

In this article, a set of RFID tags has been modeled by a set of randomly distributed half-wave dipoles. Total mono-static RCS in the direction of incident field has been computed to account for the total backscattering from the set of scattering elements (dipoles). We have shown that the two NEC-based methods can be employed to compute the RCS of randomly distributed dipoles, which is further validated by performing measurements in the anechoic chamber. Different dipole configurations were studied to analyze the distortion in RCS by varying the position and density of dipoles. The results show that when the target dipoles are randomly distributed, the deformation of the RCS is also random. Given the position and orientation of the dipoles, the corresponding distortion is difficult to predict using a purely deterministic approach and must be evaluated statistically, especially in the case of a set of strongly coupled dipoles. This requires a statistical model that can take into account the random aspect of the scenario to better analyze the RCS of a set of RFID tags in a high density context.

In ongoing works, RCS of commercial RFID tags will

be measured in the UHF RFID frequency band. The measurements will also be extended to obtain the mono-static RCS in two other planes of interest which are discussed in section 3, i.e.  $\phi = 0^\circ$  and  $\theta = 90^\circ$  planes. Further, in order to get closer to a realistic scenario, the next step would be to study the differential RCS ( $\Delta$ RCS) to model the response of an RFID tag while its impedance switches between two states [9]. Then, it would be an interesting parameter to compare the dipoles and tags in terms of  $\Delta$ RCS. As the differential RCS is a key parameter to estimate the quality of an RFID communication link, the statistics of this output would be interesting to be established and analyzed. Consequently, in long term, this study could give a reliable prediction of an RFID system's performance comprising tags in a high-density context.

## References

- [1] S. A. Ahson and M. Ilyas, *RFID handbook: Applications, Technology, Security, and Privacy*. CRC press, 2017.
- [2] P. V. Nikitin and K. S. Rao, "Theory and measurement of backscattering from RFID tags," *IEEE Antennas and Propagation Magazine*, vol. 48, no. 6, pp. 212–218, 2006.
- [3] G. Marrocco, "RFID grids: Part I—Electromagnetic theory," *IEEE Transactions on Antennas and Propagation*, vol. 59, no. 3, pp. 1019–1026, 2011.
- [4] K. Penttilä, M. Keskilammi, L. Sydänheimo, and M. Kivikoski, "Radar cross-section analysis for passive RFID systems," *IEE Proceedings-Microwaves, Antennas and Propagation*, vol. 153, no. 1, pp. 103–109, 2006.
- [5] D. Hotte, R. Siragusa, Y. Duroc, and S. Tedjini, "Radar cross-section measurement in millimetre-wave for passive millimetre-wave identification tags," *IET Microwaves, Antennas & Propagation*, vol. 9, no. 15, pp. 1733–1739, 2015.
- [6] I. Adjali, A. Gueye, S. Mostarshedi, B. Poussot, F. Nadal, and J.-M. Laheurte, "Matching evaluation of highly coupled dipoles quantified by a statistical approach," *IEEE Transactions on Antennas and Propagation*, vol. 68, no. 7, pp. 5044–5051, 2020.
- [7] F. Babaeian and N. C. Karmakar, "Time and frequency domains analysis of chipless RFID back-scattered tag reflection," *IoT*, vol. 1, no. 1, pp. 109–127, 2020.
- [8] V. Kabourek, "Objects characterization by means of wideband signals," Ph.D. dissertation, České vysoké učení technické v Praze, 2017.
- [9] P. V. Nikitin, K. Rao, and R. D. Martinez, "Differential RCS of RFID tag," *Electronics Letters*, vol. 43, no. 8, pp. 431–432, 2007.